A Fast EM Simulator for the Wideband Analysis of Multiconductor Buses for MMIC's and High-Speed Digital Circuits

M. Bressan, G. Conciauro, P. Gamba

Department of Electronics, University of Pavia
Via Ferrata 1, I-27100 PAVIA, Italy
E-mail: emgroup@ipvmv6.unipv.it

Abstract

The paper presents a new EM simulator for the analysis of multiconductor/multilayer transmission lines, applicable up to frequencies well above the range of validity of conventional quasi-TEM approaches. In reasonably short computing times the simulator yields the dispersion of the transmission-line modes, various types of characteristic impedance matrices and reveals the occurrance of higher mode propagation. Some examples demonstrate the flexibility and the efficiency of the simulator.

Introduction

Recently we got ready a very efficient EM simulator for the multimode analysis of any lossless guiding structure of the type shown in Fig. 1. This type of structures is characterized by the possibility of decomposing the cross section into rectangular regions layered in the y-direction only (regions $1, 2, \ldots$ in the figure). The structure can include N internal conductors of finite or infinitesimal thickness, so that the said simulator can be used in the study of nearly all the multiconductor lines used in MMIC's or in high-speed logical IC's.

The simulator is based on a novel full-wave method [1], named "Boundary Integral-Resonant Mode Expansion (BI-RME) Method". By this method it is possible to obtain in reasonably short times the dispersion of all the modes that propagate up to some given frequency, in particular the N coupled-line modes. After giving an outline of BI-RME method, we show how the results of the mode computation can be processed to yield, with a negligible computational work, the circuit characterization of the multiconductor system in the form of the various characteristic impedances matrices described in [2],[3]. The operation of the simulator is described and some examples are presented to demonstrate its flexibility and rapidity.

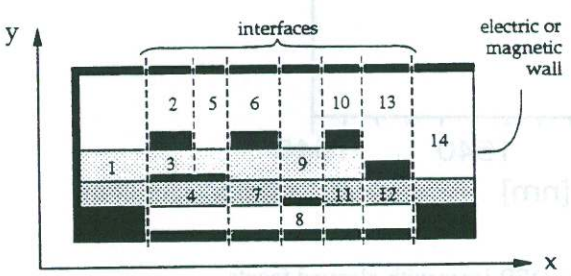

Fig. 1. Transverse section of a generic multilayer-multiconductor structure. Conductors in black.

Outline of the BI-RME method

The structure is segmented into Elementary Waveguides (EWGs) by the insertion of magnetic walls which isolate the regions 1, 2, ... The field, which propagates with a given phase constant $\beta > 0$, is considered as the effect of pairs of opposite equivalent currents $\pm\vec{J}^+$, $\pm\vec{J}^-$ (Fig.2) propagating with the same phase constant at some unknown frequency $\omega = \omega(\beta)$. The propagating frequencies of the modes are found as those values of ω for which the tangential electric fields of the various EWGs match at the two sides of each magnetic wall.

The propagating factor $\exp j(\omega t - \beta z)$ is understood so that the field is studied as a function of x , y only. The EWG field is represented by the so called BI-RME representation:

$$\vec{E} = -\nabla V - j\omega\vec{A} + \omega^2 \sum_i \frac{a_i\,\vec{e}_i}{\omega_i^2} \qquad (1)$$

$$\vec{H} = \frac{\nabla \times \vec{A}}{\mu} + \frac{j\omega}{\mu} \sum_i \frac{a_i\,\nabla \times \vec{e}_i}{\omega_i^2} \qquad (2)$$

where: $\nabla = \nabla_{xy} - j\beta\vec{u}_z$; $V = V(x, y, \beta)$ is the *quasi-static* scalar potential generated by the surface charge densities $\rho^{\pm}$ associated to $\vec{J}^{\pm}$; $\vec{A}$ is the *quasi-static* vector potential generated by $\vec{J}^{\pm}$; the vectors $\vec{e}_i = \vec{e}_i(x, y, \beta)$ represent the normalized electric field of the LSM and LSE modes of the EWG, all considered with the phase constant β and, consequently, at some well-defined (transverse resonant) frequencies $\omega_i = \omega_i(\beta)$: a_i are unknown coefficients (mode amplitudes).

The quasi-static potentials are related to their sources by boundary integrals involving ω-independent Green's

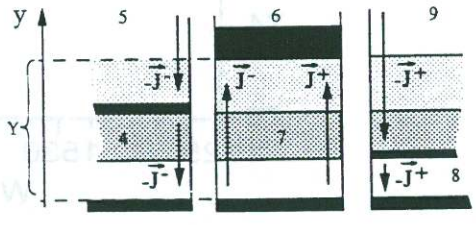

Fig. 2. The EWG corresponding to region n.7. The EWG contains three layers and is bounded by magnetic walls (at the left and the right) and by electric walls (at the top and the bottom). The EWG fields are generated by pairs of opposite equivalent currents, placed on both sides of each interface.

functions, that are known for any EWG [1]. Therefore, labeling with the superscript - (+) quantities taken on the left (right) boundary of the EWG, we can write for each EWG equations of the type:

$$\vec{E}_{tan}^{\pm} = -\nabla_{yz}\left(\mathcal{V}_{+}^{\pm}\rho^{+} + \mathcal{V}_{-}^{\pm}\rho^{-}\right) + j\omega(\mathcal{A}_{+}^{\pm}\vec{J}^{+} + \mathcal{A}_{-}^{\pm}\vec{J}^{-}) + \omega^2 \sum_i \frac{a_i\, \vec{e}_i^{\pm}{}_{tan}}{\omega_i^2} \quad (3)$$

where: $\nabla_{yz} = \vec{u}_y \partial/\partial y - j\beta\vec{u}_z$ is the tangential component of ∇; $\rho = -(\nabla_{yz}\cdot\vec{J})/j\omega$ is the charge density; the symbols $\mathcal{V}_{\pm}^{\pm}$ and $\mathcal{A}_{\pm}^{\pm}$ are frequency-independent linear operators relating surface fields defined over the same or opposite boundaries, that represent V and the tangential component of $\vec{A}$ in the form of boundary integrals.

Furthermore the mode amplitudes are related to the currents by equations of the type:

$$(\omega_i^2 - \omega^2)\, a_i = -j\omega \int_Y (\vec{e}_i^{+}\cdot\vec{J}^{+} + \vec{e}_i^{-}\cdot\vec{J}^{-})\, dy \quad (4)$$

where Y represents the y-interval spanned by the EWG (see Fig. 2).

Should the mode amplitudes be eliminated between (3) and (4), the form assumed by the expression of the electric field would reveal that the asymptotic behavior of the elements of the mode expansion is dictated by the factor ω_i^{-4}. Therefore, the mode expansion converges rapidly enough for being truncated starting from terms with ω_i not much larger than the maximum value of ω in the band of interest. In transmission line analysis, the number of the modes to be retained is of the order of unity in most cases, because the EWGs are normally so small that all their modes propagate at frequencies well above the band of interest (the only exception is the "parallel plate" LSM mode, whose propagating frequency becomes smaller and smaller with decreasing β).

The equivalent currents and charges over each interface (see Fig. 1) are approximated by expressions of the type:

$$\vec{J} = -j\omega \sum_{r=1}^{R} q_r \vec{v}_r + \sum_{r=0}^{R} i_r \vec{w}_r \quad (5)$$

$$\rho = \sum_r q_r \frac{db_r}{dy} \quad (6)$$

where q_r and i_r are unknown coefficients, the functions $b_r = b_r(y)$ are scalar basis functions defined over the interface and $\vec{v}_r$, $\vec{w}_s$ are given by:

$$\vec{v}_r = b_r \vec{u}_y \quad (7)$$

$$\vec{w}_r = \beta b_r \vec{u}_y - j\frac{db_r}{dy} \quad (r \neq 0) \quad (8)$$

$$\vec{w}_0 = \kappa \vec{u}_y \quad (\kappa = cost.) \quad (9)$$

Note that $\nabla_{yz}\cdot\vec{w}_r = 0$, $\nabla_{yz}\cdot\vec{v}_r \neq 0$.

Matching the tangential electric fields at all the interfaces by the Galerkin's method (i.e., using $\vec{v}_r$ and $\vec{w}_r$ for testing), we obtain two algebraic systems of linear equations involving the q- and the i- variables (for all the interfaces) and the a-variables (for all the EWGs). A further system relating the same variables is obtained by substituting the approximants of the currents into (4), written for all the modes of all the EWGs. The structure of (3) and (4) reveals at glance that in all the said equations the frequency appears only through the multiplicative factors $j\omega$ and ω^2.

It turns out that the system obtained from testing with the solenoidal functions $\{\vec{w}\}$ permits to express the i-variables in terms of the others, by a matrix equation of the type:

$$\mathbf{i} = j\omega(\mathbf{D}^{(\beta)}\,\mathbf{q} + \mathbf{E}^{(\beta)}\,\mathbf{a}) \quad (10)$$

where the matrices $\mathbf{D}^{(\beta)}$ and $\mathbf{E}^{(\beta)}$ depend on β, not on ω. Furthermore it turns out that eliminating the i-variables from the other two systems the problem of the mode determination reduces to the solution of a *linear* matrix eigenvalue equation of the type:

$$\mathbf{M}^{(\beta)} \begin{bmatrix} \mathbf{q} \\ \mathbf{a} \end{bmatrix} = \omega^{-2} \begin{bmatrix} \mathbf{F}^{(\beta)} & \mathbf{0} \\ \mathbf{0} & \mathbf{1} \end{bmatrix} \begin{bmatrix} \mathbf{q} \\ \mathbf{a} \end{bmatrix} \quad (11)$$

Note that the only meaningful eigenvalues ω are those below the maximum frequency of interest ω_{max}, since the approximations due to the truncation of the modal series were assumed to be acceptable only in this range. These eigenvalues, denoted by $\omega_1^{(\beta)}, \omega_2^{(\beta)}, \ldots, \omega_M^{(\beta)}$, represent frequencies at which the lowest M-modes of the structure propagate with the phase constant β. Assuming N internal conductors and considering sufficiently low values of β, we find $M \geq N$ modes propagating in the band of interest, the first N of which are the coupled-line modes of the structure. For any mode the eigenvectors $(\mathbf{q}_m^{(\beta)}, \mathbf{a}_m^{(\beta)})$ and the corresponding vectors $\mathbf{i}_m^{(\beta)}$ obtained from (10) permit to calculate the charge and current densities at all interfaces, via (5) and (6). Thus, the magnetic field can be obtained at any point of interest in each EWG using (2), so that the current densities over the conductors can be calculated easily. Then, integrating over the surfaces of the N internal conductors, it is easy to find the current vector for the m-th mode:

$$\mathbf{I}_m^{(\beta)} = \left(I_{1m}^{(\beta)}, I_{2m}^{(\beta)} \ldots I_{Nm}^{(\beta)}\right)^T \quad (12)$$

Furthermore it can be shown that the energy per unit lenght of the m-th mode is given by:

$$W_m^{(\beta)} = \frac{1}{2}\left(\tilde{\mathbf{q}}_m^{(\beta)}\mathbf{F}^{(\beta)}\,\mathbf{q}_m^{(\beta)} + \tilde{\mathbf{a}}_m^{(\beta)}\mathbf{a}_m^{(\beta)}\right) \quad (13)$$

where the tilde denotes the transpose.

Calculation of characteristic impedances

We repeat the calculation of $\omega_m^{(\beta)}$, $W_m^{(\beta)}$, $\mathbf{I}_m^{(\beta)}$ for increasing values of β, starting from values small enough to find N modes at least propagating below ω_{max} and stopping at values where no propagating mode is found.

In this way we obtain sufficient data for interpolating the phase constant $\beta_m^{(\omega)}$, the energy p.u.l. $W_m^{(\omega)}$ and the current vector $\mathbf{I}_m^{(\omega)}$ for all the coupled-line modes at any given frequency $\omega < \omega_{max}$. Furthermore we can determine the mode-powers at the frequency ω using the expression:

$$P_m^{(\omega)} = W_m^{(\omega)} \frac{d\,\omega}{d\beta_m^{(\omega)}}$$

where the derivative represents the group velocity. From these power-current data we can deduce the various types of characteristic impedances used in multiconductor transmission line theory. The so-called "modal characteristic impedance matrix" [2] is given by :

$$\mathbf{Z}_c^{(\omega)} = \mathrm{diag}\left\{ \frac{2\,P_m^{(\omega)}}{\| \mathbf{I}_m^{(\omega)} \|^2} \right\} \tag{14}$$

The elements of the so-called "line-mode impedance matrix" (i.e., the voltage/current ratio in the i-th conductor for the m-th mode [3]) are given by:

$$Z_{im}^{(\omega)} = \frac{2P_m^{(\omega)} (\tilde{\mathbf{I}}^{(\omega)^{-1}})_{im}}{I_{im}^{(\omega)}} \tag{15}$$

where $\mathbf{I}^{(\omega)}$ is the $N \times N$ matrix whose columns are the current vectors of the coupled-line modes. all considered at the same frequency: $\mathbf{I}^{(\omega)} = (\mathbf{I}_1^{(\omega)}, \mathbf{I}_2^{(\omega)}, \ldots . \mathbf{I}_N^{(\omega)})$.

Finally the "characteristic impedance matrix" [2] is given by:

$$\mathbf{Z}^{(\omega)} = 2\tilde{\mathbf{I}}^{(\omega)^{-1}} \mathrm{diag}\{P_m^{(\omega)}\}\, \mathbf{I}^{(\omega)^{-1}} \tag{16}$$

The simulator

The described algorithm has been implemented in a numerical simulator running on a Digital Alphastation $200^{4/233}$. The simulator accepts as input the geometrical, positional and physical data of the EWGs and automatically determines the set of interfaces with all the informations about the EWGs separated by each of them.

The basis functions b_r appearing in (5)-(8) are triangular splines (see [1] for more details). For each interface, their number and their location are specified by the operator. The simulator starts running after the maximum frequency of interest, the starting value of β, the step $\Delta\beta$ and a parameter $\zeta > 1$ (specified just below) are given. For a given value of β the calculation consists of the following parts.

I - *Determination of the modes of the EWGs* - For each EWG the simulator determines the LSM and LSE modes to be retained in the mode expansion (3). The modes are determined as the eigensolutions of appropriate Sturm-Liouville equations, considering only the eigenfrequencies $\omega_i < \zeta\omega_{max}$. Therefore, for a given ω_{max} the number of terms retained in the mode expansions for the various EWGs (i.e., the size of the vector **a**) is the larger

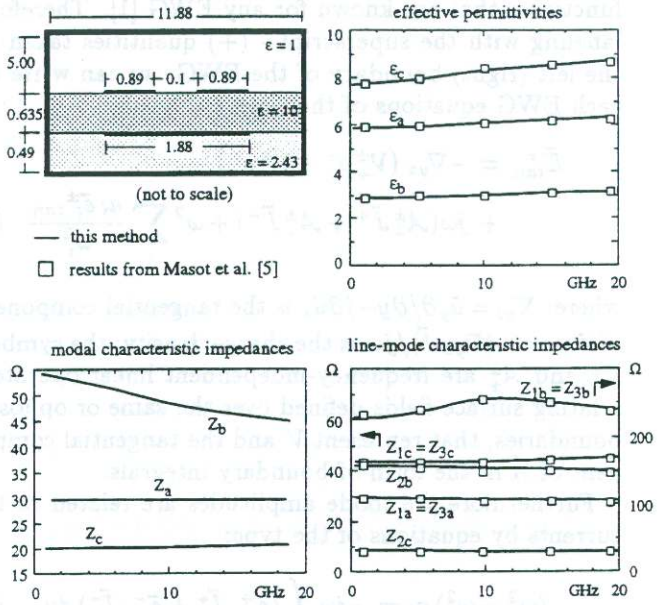

Fig. 3. Results for a three-microstrip directional coupler. The subscripts a, b, c denote the three coupled-line modes, the subscripts 1, 3 the upper strips, the subscript 2 the lower one. Even and odd modes were calculated separately. The results compare well with those reported in [5] for the same structure, without the shield. We used 40 q-variables and 17 a-variables. The CPU time was 0.6 sec for each value of β, on a Digital Alphastation 200.

the higher is the value assigned to ζ (tipically $\zeta = 2.5$ is sufficient for attaining an acceptable accuracy).

II - *Matrix calculation* - The simulator determines the matrices involved in (10) and (11). Though the matrix elements originating from the Galerkin's method can be expressed by sums of integrals that can be evaluated analytically [1], the number of these integrals is very large and makes this part of the calculation to take a large part of the CPU time. Other matrix manipulations are trivial and require a negligible time.

III - *Solution of the eigenvalue problem* - It can be shown that the matrices on both sides of (11) are real-symmetric and positive-definite. Furthermore, only the eigensolutions with $\omega < \omega_{max}$ are of interest, whose number is typically small (of the order of the number N of the internal conductors). Then the solution of (11) can be performed in short times, using very efficient library routines [4]. With these routines the eigenvectors are typically normalized in such a way as the energy (13) is equal to 1/2. If no eigenvalue $\omega < \omega_{max}$ is found the calculation is stopped, since this means that the current value of β is too large for having mode propagation in the band of interest.

IV - *Evaluation of the currents* - For any mode the current intensity in an internal conductor consists of the contribution of the currents flowing over the surfaces parallel to x, z and of the contribution of the currents flowing on the surfaces parallel to y, z (if the conductor has a finite tickness). The second contribution is deduced from (5), directly, since the current densities on the lateral sides of the conductors are opposite to the

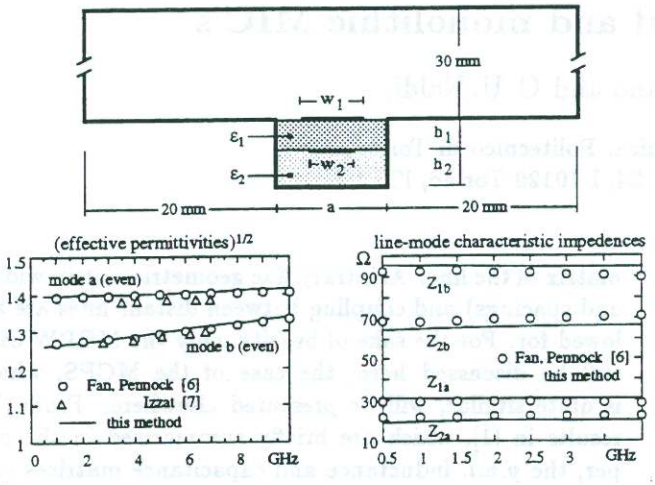

Fig. 4. Results for a strip inset dielectric guide. The subscripts a, b refer to the first and the second even mode respectively, the subscripts 1, 2 to the upper and the lower strips. Even modes where calculated considering half structure and a magnetic wall in the symmetry plane. The effective permittivities have been calculated considering $\epsilon_1 = \epsilon_2 = 2.04, a = 22.86mm, h_1 = 2.16mm, h_2 = 8mm, w_1 = 5mm, w_2 = 10mm$. The line-mode impedences have been calculated with: $\epsilon_1 = 4.7\epsilon_2 = 2.04, a = 10.16mm, h_1 = 2.54mm, h_2 = 12.7mm, w_1 = 7mm, w_2 = 5mm$. The results compare well with those reported in [6] and [7]. for the same structure without the upper part of the shielding. We used 380 q-variables and 53 a-variables. The CPU time was 22 sec for each value of β, on a Digital Alphastation 200.

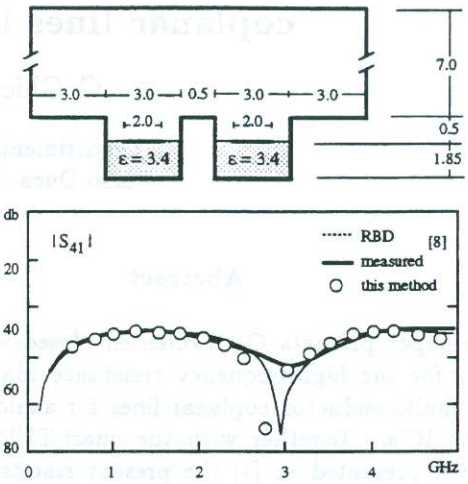

Fig. 5. Cross-talk between two buried microstrip lines. All dimensions are in mm. The value of $\mid S_{41} \mid$ refers to the directional coupler considered in [8]. It was deduced from the dispersion characteristics, the modal characteristic impedances and the mode-current vectors calculated by the BI-RME method. The results compare very well with the experimental and calculated results reported in [8]. We used 320 q-variables and 5 a-variables. The CPU time was 19 sec for each value of β, on a Digital Alphastation 200.

equivalent currents considered on the other side of the interface adhering to the conductor. The first contribution is obtained by integration of $J_z = \pm H_x$, obtained from the BI-RME representation (2) of the magnetic field in the EWGs placed above and below the considered conductor. The integration is trivial so that the computation of the current vectors (12) requires a negligible time.

The results of these calculations are stored in the memory. Then, for any given frequency in the band of interest, the simulator extrapolates the phase constants, the effective permittivities of the modes ($\epsilon_m = (\beta_m c/\omega)^2$) and the characteristic impedance matrices (14), (15), (16). The output consists in a formatted file including these results.

Some examples illustrating the flexibility and the rapidity of the simulator are described in Fig. 3 to 6. In particular the case considered in Fig. 6 indicates the effectiveness of the method in the study of buses including large numbers of conductors.

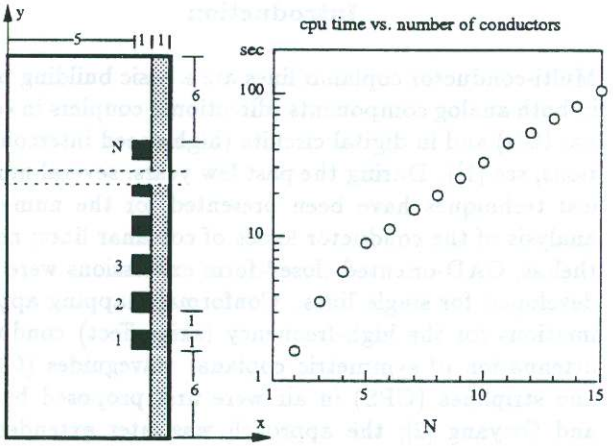

Fig. 6. N square-conductor bus. The plot gives an idea of the increase of the CPU time with increasing the number of the conductors. The CPU time refers to the calculation of the N coupled-line modes for a single value of β, on a Digital Alphastation 200.

References

[1] M. Bressan, G. Conciauro, P. Gamba, "Analysis of Guided Modes in Multilayer/Multiconductor Structures by the Boundary Integral - Resonant Mode Expansion Method", *IEEE Trans. on Microwave Theory Tech.*, vol. 44, n. 5, May 1996.

[2] G. G. Gentili, M. Salazar-Palma, 'The Definition and Computation of Modal Characterisctic Impedance in quasi-TEM Coupled Transmission Lines", *IEEE Trans. on Microwave Theory Tech.*, vol. 43, n. 2, Feb. 1995, pp. 338-343.

[3] V. K. Tripathi, H. Lee, 'Spectral Domain Computation of Characteristic Impedences and Multiport parameters of Multiple Coupled Microstrip Lines", *IEEE Trans. on Microwave Theory Tech.*, vol. 37, n. 1, Jan. 1989, pp. 215-221.

[4] E. Anderson et al., "LAPACK, User's Guide", *SIAM*, Philadelphia, 1992.

[5] F. Masot, F. Medina, M. Horno, 'Analysis and Experimental Validation of a Type of Three-Microstrip Directional Coupler, *IEEE Trans. on Microwave Theory Tech.*, vol. 42, pp.1624-1631, Sept. 1994.

[6] Z. Fan, S. R. Pennock: 'Broadside Strip Inset Dielectric Guide and its Directional Coupler Application, *IEEE Trans. on Microwave Theory Tech.*, vol. 43, No. 3, pp. 612-619, March 1996.

[7] N. Izzat: 'Space Domain Analysis of Inhomogeneous Waveguides of the Microstrip and Inset Guide Families, *Ph.D dissertation.*, Bath University, 1991.

[8] T. Ishikawa, E. Yamashita, "Experimental Results on Buried Microstrip Lines for Constructing High-Density Microwave Integrated circuits", *IEEE Microwave and Guided Wave Letters*, vol. 5, n. 12, pp. 437-438, Dec. 1995.